Inorg. Chem. **2006**, *45*, 5187–5195

Construction of New Heteroselenometallic Clusters: Formation of Crownlike $[Et_4N]_4[(\mu_5\text{-}WSe_4)(CuI)_5(\mu\text{-}I)_2]$ and Octahedral Polymeric $[(\mu_6\text{-}WSe_4)Cu_6I_4(py)_4]_n$ from Planar $[Et_4N]_4[(\mu_4\text{-}WSe_4)Cu_4I_6]$ with Additional Faces

Qian-Feng Zhang,*,† Zhan Yu,† Jihai Ding,† Yinglin Song,‖ Alexander Rothenberger,§ Dieter Fenske,§ and Wa-Hung Leung‡

Department of Applied Chemistry, Anhui University of Technology, Maanshan, Anhui 243002, P. R. China, Department of Chemistry, The Hong Kong University of Science and Technology, Clear Water Bay, Kowloon, Hong Kong, P. R. China, Institut für Anorganische Chemie, Universität Karlsruhe (TH), 76128 Karlsruhe, Germany, and Department of Physics, Harbin Institute of Technology, Harbin 150001, P. R. China

Received January 29, 2006

The coplanar cluster compound $[Et_4N]_4[(\mu_4\text{-}WSe_4)Cu_4I_6]$ (**1**) was prepared from reaction of $[Et_4N]_2[WSe_4]$ with 4 equiv of CuI in *N,N*-dimethylformamide (DMF) solution in the presence of $[Et_4N]I$. Treatment of **1** with pyridine (py) in dry MeCN gave the neutral cluster $[(\mu_4\text{-}WSe_4)Cu_4(py)_6I_2]$ (**2**) in good yield. Recrystallization of **1** from py/*i*-PrOH resulted in the reorganization of the coplanar WSe_4Cu_4 core and the formation of a neutral polymeric cluster $[(\mu_3\text{-}WOSe_3)Cu_3(py)_3(\mu\text{-}I)]_n$ (**3**) containing a nest-shaped $OWSe_3Cu_3$ core and a terminal W═O bond. The interaction of cluster **1** with excess PPh_3 in CH_2Cl_2 gave $[(\mu_3\text{-}WSe_4)Cu_3(PPh_3)_3(\mu_3\text{-}I)]$ (**4**) which has a cubanelike $SeWSe_3Cu_3I$ core. Treatment of **1** with 1 equiv of CuI in dimethyl sulfoxide (DMSO) yielded $[Et_4N]_4[(\mu_5\text{-}WSe_4)(CuI)_5(\mu\text{-}I)_2]$ (**5**) which has a crownlike core structure. Treatment of **1** in DMF with 2 equiv of CuI in the presence of py resulted in the formation of a two-dimensional polymeric cluster, $[(\mu_6\text{-}WSe_4)Cu_6I_4(py)_4]_n$ (**6**), consisting of an octahedral WSe_4Cu_6 repeating unit. The solid-state structures of clusters **3**, **5**, and **6** have been further established by X-ray crystallography. The nonlinear optical properties of **6** have been also investigated. Cluster **6** was found to exhibit good photostability and a large optical limiting effect with the limiting threshold being ca. 0.3 J cm^{-2}.

Introduction

The chemistry of heterothiometallic clusters containing $[MS_4]^{2-}$ (M = Mo, W) has been well developed because of their significances in biological systems and their rich reaction and structural chemistry.[1−3] Since the discovery that heterothiometallic clusters exhibit strong third-order nonlinear optical properties (NLO) about 10 years ago,[4] a number of such clusters with various structural types have been synthesized by both solution and solid-state methods,[5] and their NLO properties have been studied.[6] The chemistry of

* To whom correspondence should be addressed. E-mail: zhangqf@ahut.edu.cn.

† Anhui University of Technology.

‡ The Hong Kong University of Science and Technology.

§ Universität Karlsruhe (TH).

‖ Harbin Institute of Technology.

(1) (a) Venkateswara Rao, P.; Holm, R. H. *Chem. Rev.* **2004**, *104*, 527. (b) Lee, S. C.; Holm, R. H. *Chem. Rev.* **2004**, *104*, 1135. (c) Malinak, S. M.; Coucouvanis, D. *Prog. Inorg. Chem.* **2001**, *49*, 599. (d) Holm, R. H. *Adv. Inorg. Chem.* **1992**, *38*, 1. (e) Coucouvanis, D. *Acc. Chem. Res.* **1991**, *24*, 1. (f) Holm, R. H.; Berg, J. *Acc. Chem. Res.* **1986**, *19*, 363. (g) Müller, A.; Diemann, E.; Jostes, R.; Bögge, H. *Angew. Chem., Int. Ed. Engl.* **1981**, *20*, 934.

(2) (a) *Transition Metal Sulfur Chemistry*: *Biological and Industrial Significance*; Stiefel, E. I., Matsumoto, K., Eds.; American Chemical Society: Washington, DC, 1996. (b) Lang. J. P.; Jiao, C. M.; Qian, S. B.; Zhang, W. H.; Abrahams, B. F. *Inorg. Chem.* **2005**, *44*, 3664. (b) Li, Z. H.; Du, S. W.; Wu, X. T. *Inorg. Chem.* **2004**, *43*, 4776. (c) Zhuo, H. C.; Holm, R. H. *Inorg. Chem.* **2003**, *42*, 2478. (d) Zhang, Y.; Zuo, J. L.; Zhuo, H. C.; Holm, R. H. *J. Am. Chem. Soc.* **2002**, *124*, 14292. (e) Yu, H.; Xu, Q. F.; Sun, Z. R.; Ji, S. J.; Chen, J. X.; Liu, Q.; Lang, J. P.; Tatsumi, K. *Chem. Commun.* **2001**, 2614. (f) Huang, Q.; Wu. X. T.; Sheng, T. L.; Wang, Q. M.; Lu, J. X. *Inorg. Chem.* **1995**, *34*, 4931.

(3) (a) Niu, Y. Y.; Zheng, H. G.; Hou, H. W.; Xin, X. Q. *Coord. Chem. Rev.* **2004**, *248*, 169. (b) Hou, H. W.; Xin, X. Q.; Shi, S. *Coord. Chem. Rev.* **1996**, *153*, 169. (c) Wu, X. T.; Chen, P. C.; Du, S. W.; Zhu, N. Y.; Lu, J. X. *J. Cluster Sci.* **1994**, *5*, 265.

(4) (a) Shi, S.; Ji, W.; Tang, S. H.; Lang, J. P.; Xin, X. Q. *J. Am. Chem. Soc.* **1994**, *116*, 3615. (b) Shi, S.; Ji. W.; Lang, J. P.; Xin, X. Q. *J. Phys. Chem.* **1994**, *98*, 3570.

10.1021/ic060161p CCC: $33.50
Published on Web 05/25/2006

the corresponding heteroselenometallic clusters containing $[MSe_4]^{2-}$ (M = Mo, W) has, however, received relatively less attention until recently.[7] Our interest in heteroselenometallic clusters comes from notion that these clusters would possess better NLO properties than their thiometalate congeners[8] because of the heavy atom effect (i.e., selenium being heavier than sulfur). Additionally, selenium-containing compounds have important applications, such as being precursors for low-band gap semiconductors and nonlinear optical materials.[9] With this connection, we set out to synthesize new heteroselenometallic clusters by reactions between tetraselenometalate anions and coinage-metal cations and to further to investigate the structure−property relationship of this class of NLO materials.

In contrast to their heterothiometallic analogues,[3,5,10] rational synthetic routes to heteroselenometallic clusters have not been well developed. Müller first demonstrated the formation of linear trinuclear cluster $[(\mu\text{-}WSe_4)(AgPPh_3)_2]$ by the coordination reaction of $[WSe_4]^{2-}$ and $[Ag(PPh_3)]^+$.[11] Subsequently, Ibers and Hong have exploited the interactions of $[MSe_4]^{2-}$ (M = Mo, W) with the coinage−metal cations Cu^+, Ag^+, and Au^+ and isolated a series of coinage-metal/MSe_4 compounds with structural types ranging from linear,[12] butterfly,[13] cubane,[12a,14] incomplete-cubane,[15] coplanar T-frame, open cross-frame,[16] and cage[16a] to pinwheel shapes.[17] Xin and co-workers have synthesized coplanar open polymeric clusters that exhibit large optical limiting effects and cyanide-bridged three-dimensional cross-frameworks based on WS_4/CuCN.[18]

Chart 1

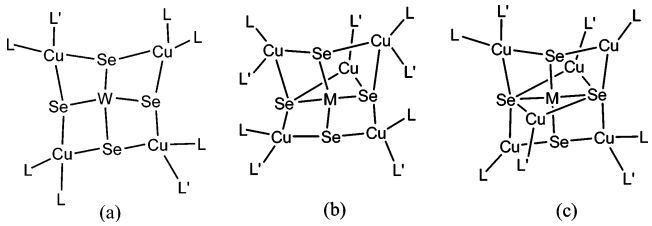

The variation of structural types for these heteroselenometallic clusters mainly depends on the number of coinage-metal atoms bound to the six MSe_2 edges of the central $[MSe_4]^{2-}$ tetrahedron. Previously, one of us investigated the influence of peripheral ligands on the reactivity and structural transformations of heteroselenometallic clusters by ^{95}Mo NMR spectroscopy.[16a] Given the fact that the coplanar MSe_4Cu_4 cluster (a) has two MSe_2 edges that can bind additional metal ions, we seek to synthesize new clusters with MSe_4Cu_5 (b) and MSe_4Cu_6 (c) cores, as shown in Chart 1 (M = Mo, W; L, L′ = ligands), by binding metal ions to these two MSe_2 edges. Herein, we report the synthesis of crownlike $[Et_4N]_4[(\mu_5\text{-}WSe_4)(CuI)_5(\mu\text{-}I)_2]$ and octahedral polymeric $[(\mu_6\text{-}WSe_4)Cu_6I_4(py)_4]_n$ by coordination of additional Cu(I) ions to the planar cluster $[Et_4N]_4[(\mu_4\text{-}WSe_4)Cu_4I_6]$. The molecular structures and spectroscopic properties along with optical nonlinearities of these clusters will be presented in this paper.

Experimental Section

Materials and Measurements. All syntheses were performed in oven-dried glassware under a purified nitrogen atmosphere using standard Schlenk techniques. The solvents were purified by conventional methods and degassed prior to use. $[Et_4N]_2[WSe_4]$ was prepared by a modification of the literature method.[19] CuI,

(5) (a) Cai, Y.; Wang, Y.; Li, Y. Z.; Wang, X. S.; Xin, X. Q.; Liu, C. M.; Zheng, H. G. *Inorg. Chem.* **2005**, *44*, 9128. (b) Liang, K.; Zheng, H. G.; Song, Y. L.; Lappert, M. E.; Li, Y. Z.; Xin, X. Q.; Huang, Z. X.; Chen, J. T.; Lu, S. F. *Angew. Chem., Int. Ed. Engl.* **2004**, *43*, 5776. (c) Li, Z. H.; Du, S. W.; Wu, X. T. *Dalton Trans.* **2004**, 2438. (d) Zheng, H. G.; Zhou, J. L.; Lappert, M. E.; Song, Y. L.; Li, Y. Z.; Xin, X. Q. *Eur. J. Inorg. Chem.* **2004**, 2754. (e) Niu, Y. Y.; Chen, T. N.; Liu, S. X.; Song, Y. L.; Wang, Y. X.; Xue. Z. L.; Xin, X. Q. *J. Chem. Soc., Dalton Trans.* **2002**, 1980. (f) Niu, Y. Y.; Song, Y. L.; Zheng, H. G.; Long, D. L.; Fun, H. K.; Xin, X. Q. *New J. Chem.* **2001**, *25*, 945. (g) Zhang, Q. F.; Niu, Y. Y.; Leung, W. H.; Song, Y. L.; Williams, I. D.; Xin, X. Q. *Chem. Commun.* **2001**, 1126.

(6) (a) Shi, S. Nonlinear Optical Properties of Inorganic Clusters. In *Optoelectronic Properties of Inorganic Compounds*; Roundhill, D. M., Fackler, J. P., Jr., Eds.; Plenum Press: New York, 1999; pp 55−105. (b) Coe, B. J. In *Comprehensive Coordination Chemistry II*; McCleverty, J. A., Meyer, T. J., Eds.; Elsevier Pergamon: Oxford, U. K., 2004; Vol. 9, pp 621−687. (c) Zhang, C.; Song, Y. L.; Kuhn, F. E.; Wang, Y. X.; Xin, X. Q.; Hermann, W. A. *Adv. Mater*. **2002**, *14*, 818. (d) Shi, S.; Lin, Z.; Mo, Y.; Xin, X. Q. *J. Phys. Chem*. **1996**, *100*, 10696.

(7) (a) Zhang, Q. F.; Leung, W. H.; Xin, X. Q. *Coord. Chem. Rev.* **2002**, *224*, 35. (b) Zhang, Q. F.; Xiong, Y. N.; Lai, T. S.; Ji, W.; Xin, X. Q. *J. Phys. Chem. B* **2000**, *104*, 3446.

(8) (a) Coe, B. J.; Curati, N. R. M. *Comments Inorg. Chem.* **2004**, *25*, 147. (b) Wachter, J. *Eur. J. Inorg. Chem.* **2004**, 1367. (c) Feliz, M.; Garriga, J. M.; Llusar, R.; Uriel, S.; Humphrey, M. G.; Lucas, N. T.; Samoc, M.; Luther-Davies, B. *Inorg. Chem.* **2002**, *40*, 6132. (d) Xiong, Y. N.; Ji, W.; Zhang, Q. F.; Xin, X. Q. *J. App. Phys*. **2000**, *88*, 1225.

(9) See any issue of The Bulletin of the Selenium−Tellurium Development Association, Grimbergen, Belgium, 1991.

(10) (a) Zhang, W.; Behrens, A.; Gatjens, J.; Ebel, M.; Wu, X.; Rehder, D. *Inorg. Chem.* **2004**, *43*, 3020. (b) Chen, L.; Yu, H.; Wu, L. M.; Du, W. X.; Gao, X. C.; Lin, P.; Zhang, W. J.; Cui, C. P.; Wu, X. T. *J. Solid State Chem.* **2000**, *151*, 286. (c) Guo, J.; Sheng, T. L.; Zhang, W. J.; Wu, X. T.; Lin, P.; Wang, Q. M.; Lu, J. X. *Inorg. Chem*. **1998**, *37*, 3689. (d) Lin, P.; Wu, X. T.; Huang, Q.; Sheng, T. L.; Zhang, W. J.; Guo, J.; Lu, J. X. *Inorg. Chem*. **1998**, *37*, 5672.

(11) Müller, A.; Bögge, H.; Schimanski, J.; Penk, M.; Nieradzik, K.; Dartmann, D.; Krickemyer, E.; Schimanski, J.; Römer, C.; Römer, M.; Dornfeld, H.; Wienböker, U.; Hellmann, W.; Zimmermann, M. *Monatsch. Chem*. **1989**, *120*, 367.

(12) (a) Christuk, C. C.; Ansari, M. A.; Ibers, J. A. *Inorg. Chem*. **1992**, *31*, 4365. (b) Christuk, C. C.; Ibers, J. A. *Inorg. Chem.* **1993**, *37*, 5105. (c) Salm, R. J.; Ibers, J. A. *Inorg. Chem*. **1994**, *33*, 4216. (d) Salm, R. J.; Misetic, A.; Ibers, J. A. *Inorg. Chim. Acta* **1995**, *240*, 239. (e) Zhang, Q. F.; Cao, R.; Hong, M. C.; Wu, D. X.; Zhang, W. J.; Zheng, Y.; Liu, H. Q. *Inorg. Chim. Acta* **1998**, *271*, 93. (f) Zhang, Q. F.; Leung, W. H.; Song, Y. L.; Hong, M. C.; Kennard, C. L.; Xin, X. Q. *New J. Chem.* **2001**, *25*, 465.

(13) Wang, Q. M.; Wu. X. T.; Huang, Q.; Sheng, T. L.; Lin, P. *Polyhedron* **1997**, *16*, 1439.

(14) (a) Ansari, M. A.; Bollinger, J. C.; Christuk, C. C.; Ibers, J. A. *Acta Crystallogr*. **1994**, *C50*, 869. (b) Du, S. W.; Wu, X. T.; Lu, J. X. *Polyhedron* **1994**, *12*, 841. (c) Zhang, Q. F.; Hong, M. C.; Su, W. P.; Cao, R.; Liu, H. Q. *Polyhedron* **1997**, *16*, 1433. (d) Zhang, Q. F.; Hong, M. C.; Liu, H. Q. *Transition Met. Chem*. **1997**, *22*, 156. (e) Yao, W. R.; Song, Y. L.; Xin, X. Q.; Zhang, Q. F. *J. Mol. Struct.* **2003**, *655*, 391.

(15) Hong, M. C.; Wu, M. H.; Huang, X. Y.; Jiang, F. L.; Cao, R.; Liu, H. Q.; Lu, J. X. *Inorg. Chim. Acta* **1997**, *260*, 73.

(16) (a) Hong, M. C.; Zhang, Q. F.; Cao, R.; Wu, D. X.; Chen, J. T.; Zhang, W. J.; Liu, H. Q.; Lu, J. X. *Inorg. Chem.* **1997**, *36*, 6251. (b) Zhang, Q. F.; Bao, M. T.; Hong, M. C.; Cao, R.; Song, Y. L.; Xin, X. Q. *J. Chem. Soc., Dalton Trans.* **2000**, 605.

(17) Christuk, C. C.; Ansari, M. A.; Ibers, J. A. *Angew. Chem., Int. Ed. Engl*. **1992**, *31*, 1477.

(18) (a) Zhang, Q. F.; Leung, W. H.; Xin, X. Q.; Fun, H. K. *Inorg. Chem*. **2000**, *39*, 417. (b) Zhang, C.; Song, Y. L.; Xu. Y.; Fun, H. K.; Fang, G. Y.; Wang, Y. X.; Xin, X. Q. *J. Chem. Soc., Dalton Trans.* **2000**, 2823.

(19) O'Neal, S. C.; Kolis, J. W. *J. Am. Chem. Soc.* **1988**, *110*, 1971.

$[Et_4N]I$, PPh_3, and pyridine were purchased from Aldrich Ltd. and used without further purification. All elemental analyses were carried out using a Perkin-Elmer 2400 CHN analyzer. Electronic absorption spectra were obtained on a Shimadzu UV-3000 spectrophotometer. Infrared spectra were recorded on a Digilab FTS-40 spectrophotometer with use of pressed KBr pellets, and positive FAB mass spectra were recorded on a Finnigan TSQ 7000 spectrometer. NMR spectra were recorded on a Bruker ALX 300 spectrometer operating at 300 and 121.5 MHz for ^1H and ^{31}P, respectively, and the chemical shifts (δ, ppm) were reported with reference to $SiMe_4$ (1H) and H_3PO_4 (^{31}P).

Preparation of $[Et_4N]_4[(\mu_4\text{-}WSe_4)Cu_4I_6]$ (1). A solution of $[Et_4N]_2[WSe_4]$ (190 mg, 0.25 mmol) in DMF (15 mL) was added to a solution of CuI (191 mg, 1.00 mmol) and $[Et_4N]I$ (129 mg, 0.50 mmol) in MeCN (5 mL). The mixture was stirred at room temperature for 1 h, during which time the color gradually changed from purple to dark red. A little precipitate was removed by filtration, and a clear filtrate was obtained. Excess MeCN was added to the filtrate until a dark-red solid was formed. The solid was isolated by filtration, washed with EtOH and Et_2O, and then dried by vacuum. The pure solid of **1** may be used for further reactions. Yield: 395 mg (77%). Recrystallization on a small scale from DMF/THF (1:4) yielded the dark-red microcrystalline product. Anal. Calcd for $C_{32}H_{80}N_4Cu_4I_6Se_4W$: C, 21.56; H, 4.49; N, 3.14. Found: C, 21.84; H, 4.61; N, 3.12. UV−vis (DMF, λ_{max}/nm (ϵ/$\times 10^{-3}$ M^{-1} cm^{-1}): 322 (12.3), 387 (sh), 420 (3.51), 475 (3.88), 495 (3.71). IR (KBr, cm^{-1}): ν(W−Se) 300 (m). ^1H NMR (DMSO-d_6): δ 1.05 (t, $J = 7.6$ Hz, CH_3 in Et_4N), 2.95 (quart, $J = 8.5$ Hz, CH_2 in Et_4N). MS (FAB): *m*/*z* 1260 ([(μ_4-WSe_4)Cu_4I_6] − 1), 1133 ([(μ_4-WSe_4)Cu_4I_5] − 1), 1006 ([(μ_4-WSe_4)Cu_4I_4] − 1), 879 ([(μ_4-WSe_4)Cu_4I_3] − 1), 752 ([(μ_4-WSe_4)Cu_4I_2] − 1), 625 ([(μ_4-WSe_4)-Cu_4I] − 1), 500 ([(μ_4-WSe_4)Cu_4] + 1).

Preparation of $[(\mu_4\text{-}WSe_4)Cu_4(py)_6I_2]$ (2). A suspension of **1** (178 mg, 0.10 mmol) in MeCN (5 mL) was added to py (5 mL). The mixture was stirred for 2 h at room temperature until the solid material was entirely dissolved. The red filtrate was carefully layered with Et_2O. Red crystals of $[(\mu_4\text{-}WSe_4)Cu_4(py)_6I_2]$ (**2**) were obtained in 3 days. The product was washed with EtOH and Et_2O and dried under vacuum. Yield: 102 mg (63%). Anal. Calcd for $C_{30}H_{30}N_6Cu_4I_2Se_4W$: C, 24.31; H, 2.02; N, 5.67. Found: C, 24.62; H, 2.11; N, 5.62. UV−vis (DMF, λ_{max}/nm, $\epsilon/\times 10^{-3}$ M^{-1} cm^{-1}): 306 (10.2), 345 (7.43), 408 (4.63), 487 (3.52). IR (KBr, cm^{-1}): ν(C−N) 1164 (s), ν(W−Se) 299 (m). ^1H NMR (DMSO-d_6): δ 8.01 (t, $J = 6.2$ Hz, *para-H* in py), 8.35 (t, $J = 6.9$ Hz, *meta-H* in py), 8.92 (d, $J = 6.6$ Hz, *ortho-H* in py). MS (FAB): *m*/*z* 1482 (M^+ + 1), 1353 (M^+ − I − 1), 1226 (M^+ − 2I − 1).

Preparation of $[(\mu_3\text{-}WOSe_3)Cu_3(py)_3(\mu\text{-}I)]_n$ (3). Cluster **1** (178 mg, 0.10 mmol) was directly dissolved in py (10 mL), and the resultant solution was crystallized by layering with *i*-PrOH to obtain red plate crystals of **3** after 10 days. Yield: 58 mg (58%). Anal. Calcd for $C_{15}H_{15}N_3OCu_3ISe_3W$: C, 18.15; H, 1.51; N, 4.24. Found: C, 18.23; H, 1.57; N, 4.18. UV−vis (DMF, λ_{max}/nm, $\epsilon/\times 10^{-3}$ M^{-1} cm^{-1}): 325 (12.7), 379 (sh) (6.82), 456 (4.20). IR (KBr, cm^{-1}): ν(C−N) 1157 (s), ν(W−O) 913 (s), ν(W−Se) 300 (m). ^1H NMR (DMSO-d_6): δ 8.07 (m, *para-H* in py), 8.32 (m, *meta-H* in py), 8.86 (dd, $J = 6.8$ Hz, *ortho-H* in py). MS (FAB): *m*/*z* 992 (M^+ + 1), 863 (M^+ − I − 1).

Preparation of $[(\mu_3\text{-}WSe_4)Cu_3(PPh_3)_3(\mu_3\text{-}I)]$ (4). A solution of PPh_3 (157 mg, 0.60 mmol) in CH_2Cl_2 (15 mL) was added to a slurry of **1** (178 mg, 0.10 mmol) in DMF (5 mL), and the mixture was stirred for 6 h at room temperature. The resulting red solution was filtered to yield an orange precipitate. Dark orange crystals of $[(\mu_3\text{-}WSe_4)Cu_3(PPh_3)_3(\mu_3\text{-}I)]$ (**4**) were obtained by layering the filtrate with THF. Yield: 74 mg (46%). Anal. Calcd for $C_{54}H_{45}P_3Cu_3ISe_4W$: C, 40.39; H, 2.80. Found: C, 40.25; H, 2.77. UV−vis (CH_2Cl_2, λ_{max}/nm, $\epsilon/\times 10^{-3}$ M^{-1} cm^{-1}): 346 (5.74), 495 (sh) (3.22). IR (KBr, cm^{-1}): ν(W−Se) 318 (m), 297 (w). ^{31}P NMR (DMSO-d_6): δ 26.4. MS (FAB): *m*/*z* 1605 (M^+ + 1), 1476 (M^+ − I − 1).

Preparation of $[Et_4N]_4[(\mu_5\text{-}WSe_4)(CuI)_5(\mu\text{-}I)_2]$ (5). An equivalent of CuI (191 mg, 0.10 mmol) was added to a solution of **1** (178 mg, 0.10 mmol) in DMSO (8 mL), and then the mixture was stirred for ca. 2 h until the CuI powder was dissolved. The resulting dark red solution was stirred for an additional 1 h and subsequently filtered to remove a little brown precipitate. Slow addition of a mixture solvent of THF/*i*-PrOH (1:3) induced the crystallization of **5** as black blocks suitable for X-ray analysis. Yield: 137 mg (62%). Anal. Calcd for $C_{32}H_{80}N_4Cu_5I_7Se_4W$: C, 17.24; H, 3.59; N, 2.51. Found: C, 17.63; H, 3.46; N, 2.48. UV−vis (DMF, λ_{max}/nm, $\epsilon/\times 10^{-3}$ M^{-1} cm^{-1}): 332 (11.4), 391 (sh), 489 (4.12). IR (KBr, cm^{-1}): ν(W−Se) 298 (m), 7293 (w). ^1H NMR (DMSO-d_6): δ 1.03 (t, $J = 7.6$ Hz, CH_3 in Et_4N), 2.92 (quart, $J = 8.2$ Hz, CH_2 in Et_4N). MS (FAB): *m*/*z* 1706 ([(μ_5-WSe_4)Cu_5I_7] − 1), 1597 ([(μ_5-WSe_4)Cu_4I_6] − 1), 1470 ([(μ_5-WSe_4)Cu_5I_5] − 1), 1343 ([(μ_5-WSe_4)-Cu_5I_4] − 1), 1216 ([(μ_5-WSe_4)Cu_5I_3] − 1), 1089 ([(μ_5-WSe_4)Cu_5I_2] − 1), 962 ([(μ_5-WSe_4)Cu_5I] − 1), 836 ([(μ_5-WSe_4)Cu_5] + 1).

Preparation of $[(\mu_6\text{-}WSe_4)Cu_6I_4(py)_4]_n$ (6). A fresh solution of CuI (382 mg, 0.20 mmol) in py (2.5 mL) was added with stirring to a suspension of **1** (178 mg, 0.10 mmol) in DMF (10 mL). A dark red solution gradually formed as the solid of **1** dissolved. The resultant solution was stirred for 4 h at room temperature and filtered to obtain a dark red filtrate. Slow vapor diffusion of Et_2O produced X-ray-quality crystals of **6** as black prisms after one week. Yield: 78 mg (46%). Anal. Calcd for $C_{20}H_{20}N_4Cu_6I_2Se_4W$: C, 14.08; H, 1.17; N, 3.28. Found: C, 14.21; H, 1.19; N, 3.12. UV−vis (DMF, λ_{max}/nm, $\epsilon/\times 10^{-3}$ M^{-1} cm^{-1}): 317 (8.25), 353 (5.39), 424 (3.21), 494 (2.83). IR (KBr, cm^{-1}): ν(C−N) 1168 (s), ν(W−Se) 295 (m), 291 (w). ^1H NMR (DMSO-d_6): δ 8.02 (t, $J = 6.4$ Hz, *para-H* in py), 8.39 (t, $J = 7.2$ Hz, *meta-H* in py), 9.01 (d, $J = 6.7$ Hz, *ortho-H* in py). MS (FAB): *m*/*z* 1706 (M^+ + 1), 1577 (M^+ − I − 1), 1451 (M^+ − 2I − 1), 1324 (M^+ − 3I − 1), 1198 (M^+ − 4I).

X-ray Crystallography. The structures of **3**, **5**, and **6** were obtained by the single-crystal X-ray diffraction technique. Crystals were mounted on the tips of perfluoropolyether oil-coated glass fibers. Data were collected at 120 K on a Siemens Stoe-IPDS diffractometer (Mo Kα radiation) equipped with an imaging plate area detector and a rotating anode. All structures were solved by the use of direct methods, and refinement was performed using full-matrix least-squares methods on F^2 with the SHELXTL software package.[20] All non-hydrogen atoms were refined anisotropically. The hydrogen atoms were generated and included in the structure factor calculations with assigned isotropic thermal parameters but were not refined. The data processing and structure refinement parameters are summarized in Table 1. Atomic coordinates, complete bond distances and angles, and anistropic thermal parameters of all non-hydrogen atoms for all three clusters are available as Supporting Information.

Optical Measurements. A DMSO solution of 2.25×10^{-5} mol dm^{-3} of **6** was placed in a 1 mm quartz cuvette for optical measurements. The optical limiting characteristics along with nonlinear absorption and refraction was investigated with a linearly polarized laser light ($\lambda = 532$ nm, pulse width = 7 ns) generated from a Q-switched and frequency-doubled Nd:YAG laser. The spatial profiles of the optical pulses were nearly Gaussian. The laser

(20) Sheldrick, G. M. *SHELXTL-97*, version 5.1; Bruker AXS, Inc.: Madison, WI, 1997.

Table 1. Crystallgraphic Data and Experimental Details for $[(\mu_3\text{-}WOSe_3)Cu_3(py)_3(\mu\text{-}I)]_n$ (**3**), $[Et_4N]_4[(\mu_5\text{-}WSe_4)(CuI)_5(\mu\text{-}I)_2]$ (**5**), and $[(\mu_6\text{-}WSe_4)Cu_6I_4(py)_4]_n$ (**6**)

	3	**5**	**6**
formula	$C_{15}H_{15}N_3OICu_3Se_3W$	$C_{32}H_{80}N_4I_7Cu_5Se_4W$	$C_{20}H_{20}N_4I_4Cu_6Se_4W$
fw	991.55	2226.69	1704.93
a (Å)	8.2156(16)	23.539(5)	14.811(2)
b (Å)	8.8229(18)	10.718(2)	14.811(2)
c (Å)	15.840(3)	22.217(4)	15.595(3)
α (deg)	102.88(3)	90	90
β (deg)	97.93(3)	94.73(3)	90
γ (deg)	94.94(3)	90	90
V (Å^3)	1100.5(4)	5586.1(19)	3421.1(10)
Z	2	4	4
cryst syst	triclinic	monoclinic	tetragonal
space group	$P\bar{1}$	$C2/c$	$I\bar{4}2d$
ρ_{calcd} (g cm^{-3})	2.992	2.648	3.310
T (K)	120(2)	120(2)	120(2)
μ (mm^{-1})	14.444	10.422	14.891
F(000)	900	4104	3056
reflns	7479	19 405	13 396
independent reflns	4414	5458	1907
R_{int}	0.0657	0.0737	0.0683
R1, wR2 ($I > 2.0\sigma(I)$)	0.0581, 0.1178	0.0629, 0.1224	0.0466, 0.1175
R1, wR2 (all data)	0.0626, 0.1258	0.0716, 0.1332	0.0467, 0.1177
GOF[a]	1.023	1.008	1.108

[a] GoF = $[(\sum w|F_o| - |F_c|)^2/(N_{obsd} - N_{params})]^{1/2}$.

beam was focused with a 25 cm focal-length focusing mirror. The radius of the laser beam waist was measured to be 30 ± 5 μm (half-width at 1/e^2 maximum in irradiation). The incident and transmitted pulse energy were measured simultaneously by two Laser Precision detectors (RjP-735 energy probes) communicating to a computer via an IEEE interface,[21] while the incident pulse energy was varied by a Newport attenuator. The interval between the laser pulses was chosen to be 1 s to avoid the influence of thermal and long-term effects. The details of the setup can be found elsewhere.[22]

Results and Discussion

Syntheses. When $[Et_4N]_2[WSe_4]$ was reacted with 4 equiv of CuI in DMF solution in the presence of $[Et_4N]I$, a dark red solution, along with a small amount of brown precipitate, was gradually formed. Upon filtration and addition of excess MeCN, an analytically pure dark-red solid characterized as $[Et_4N]_4[(\mu_4\text{-}WSe_4)Cu_4I_6]$ (**1**) by IR, MS, and elemental analyses was isolated. The formation of pentanuclear cluster **1** from the coplanar WCu_4 core is not surprising because the four faces of the $[WSe_4]^{2-}$ are equally capable of coordination with Cu(I) ions. Similar heterothiometallic clusters have been synthesized from the reaction of $[NH_4]_2[MoS_4]$, CuI, and $[Et_4N]I$.[23] It is worth noting that in the present system a long reaction time will result in a lot of insoluble brown precipitate and low yield of **1**, suggestive of rapid coordination reaction of the $[WSe_4]^{2-}$ anion with Cu(I) species. Although an attempt to obtain single crystals of **1** for single-crystal X-ray diffraction was not successful, the compound has been fully characterized using spectroscopic methods and has been proven to be a useful starting material for construction of clusters based on the planar $[(\mu_4\text{-}WSe_4)Cu_4I_6]^{4-}$ anion. Scheme 1 summarizes the syntheses of new heteroselenometallic clusters derived from **1** under the various experimental conditions.

Scheme 1. Reactions and Structural Transformations of Planar $[Et_4N]_4[(\mu_4\text{-}WSe_4)Cu_4I_6]$[a]

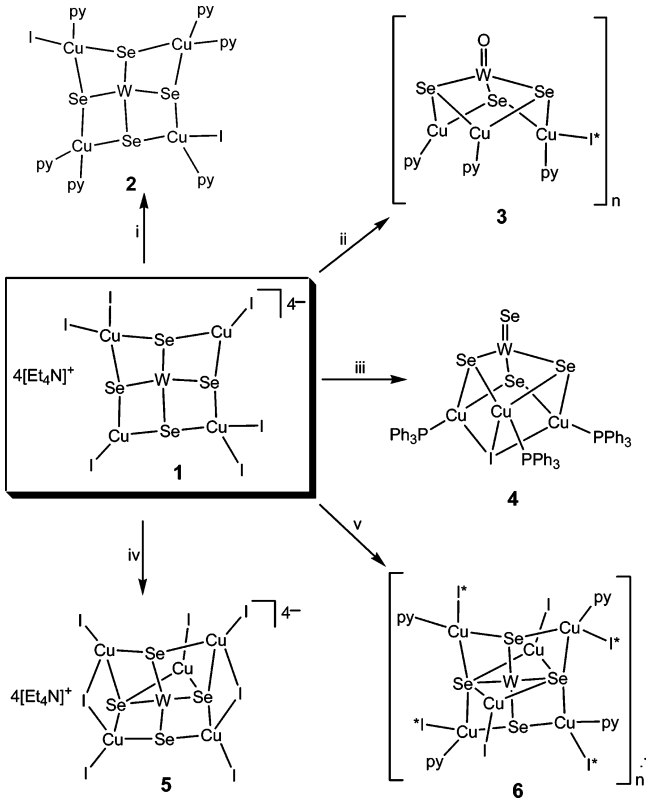

[a] Reagents and conditions: (i) py/MeCN, (ii) py/*i*-PrOH, (iii) PPh_3/DMF/CH_2Cl_2, (iv) CuI/DMSO, and (v) CuI/py/DMF.

Treatment of **1** with excess py in dry MeCN gave an orange-red solution. Slow diffusion of Et_2O into the solution gave crystals identified as $[(\mu_4\text{-}WSe_4)Cu_4(py)_6I_2]$ (**2**).[24] The

(21) (a) Sheik-Bahae, M.; Said, A. A.; Van Stryland, E. W. *Opt. Lett.* **1989**, *14*, 955. (b) Sheik-Bahae, M.; Said, A. A.; Wei, T. H.; Hagan, D. J.; Van Stryland, E. W. *IEEE J. Quantum Electron.* **1990**, *26*, 760.

(22) Hou, H. W.; Liang, B.; Xin, X. Q.; Yu, K. B.; Ge, P.; Ji, W.; Shi, S. *J. Chem. Soc., Faraday Trans.* **1996**, *92*, 2343.

(23) Lang, J. P.; Zhou, W. Y.; Xin, X. Q.; Yu, K. B. *J. Coord. Chem.* **1993**, *30*, 173.

formation of neutral **2** can be described as the replacement of four iodine atoms in **1** with py, while the coplanar WSe_4Cu_4 core structure remains unchanged. On the other hand, when cluster **1** was dissolved in neat py and crystallized from py/i-PrOH, red single crystals characterized as the one-dimensional polymeric cluster **3** with the nest-shaped repeat unit $[(\mu_3\text{-}WOSe_3)Cu_3(py)_3(\mu\text{-}I)]$ were isolated. It is believed that the driving force for the formation of the nest-shaped core of **3** from the coplanar core of **1** is the hydrolysis of the W═Se group in **1** to W═O during the recrystallization. Hydrolysis of W═Se groups to give W═O groups have been found for analogous thiometalate systems previously.[25] The cubanelike cluster $[(\mu_3\text{-}WSe_4)Cu_3(PPh_3)_3(\mu_3\text{-}I)]$ (**4**) with a nest-shaped core structure similar to that of cluster **3** was prepared by the reaction of cluster **1** with excess PPh_3 in CH_2Cl_2. This reaction involved a change of the cluster skeleton from a coplanar WSe_4Cu_4 core to the cubanelike $SeWSe_3Cu_3I$ core. In addition, the formation of the Cu−P bond resulted in the change of the binding mode for the bridged iodide ligand from μ_2 to μ_3. As previously reported, treatment of analogous coplanar clusters with PPh_3 in the presence of halides led to formation of cubane clusters. For example, treatment of $[(\mu_4\text{-}MoSe_4)Cu_4(py)_6Br_2]$ with PPh_3 produced cubanelike cluster $[(\mu_3\text{-}MoSe_4)Cu_3(PPh_3)_3(\mu_3\text{-}Br)]$, identified by ^{95}Mo NMR.[26] It may be thus understood that the cluster skeleton's transformation occurs in the reaction of cluster **1** with the coplanar WSe_4Cu_4 core because of the formation of the terminal W═O(Se) bond.

Encouraged by the above results for the reactivity of coplanar cluster **1** associated with the uncoordinated WSe_2 edges, we studied the addition reactions of cluster **1** with the Cu(I) species. Treatment of **1** in DMSO with 1 equiv of CuI resulted in the addition of 1 CuI unit and the formation of $[Et_4N]_4[(\mu_5\text{-}WSe_4)(CuI)_5(\mu\text{-}I)_2]$ (**5**), which features a crownlike core structure according to an X-ray diffraction analysis (vide infra). Efforts to synthesize other clusters using two or more equivalents of CuI failed, although apparent reactions of **1** with Cu^+ were observed. Sécheresse et al. reported that the reaction of cubanelike $[n\text{-}Pr_4N]_3[WS_4Cu_3Br_4]$ with $[Et_4N]Cl$ in CH_2Cl_2 produced an analogous thiometalate cluster $[Et_4N]_4[WS_4Cu_5Br_7]$ in a low yield.[27] In this reaction, rearrangement of the cubane $SWS_3Cu_3Br_4$ core to a crownlike $[WS_4Cu_5Br_7]^{4-}$ core was found, although the detailed mechanism by which the crownlike cluster was formed is unclear. On the other hand, treatment of **1** in DMF with 2 equiv of CuI in the presence of py produced a two-dimensional polymeric cluster, $[(\mu_6\text{-}WSe_4)Cu_6I_4(py)_4]_n$ (**6**), consisting of an octahedral WSe_4Cu_6 repeating unit. The two additional WSe_2 faces of coplanar WSe_4Cu_4 core in **1** were coordinated with two Cu atoms, resulting in coordinative saturation of the $[WSe_4]^{2-}$ tetrahedron. Previously, a $MoSe_4Cu_6$ cluster was identified as an intermediate during the transformation of $MoCu_4$ to $MoCu_{10}$ clusters by ^{95}Mo NMR spectroscopy.[16a] However, the isolation of such as an $MoSe_4Cu_6$ cluster has not yet been unsuccessful. Although analogous heterothiometallic $[MoS_4Cu_6X_4(py)_4]_n$ (X = Br, I) clusters have been synthesized by self-assembly or so-called one-pot reactions of $[Et_4N]_2[MoS_4]$ and CuX with py in a MeCN solution,[28] in this work we have clearly demonstrated that the formation of **6** involved the substitution of four iodide atoms by py and the binding of CuI moieties to the two uncoordinated WSe_2 faces in the $[WSe_4]^{2-}$ of cluster **1**. As one might expect, connecting the octahedral WSe_4Cu_6 core with the bridged iodide ligands results in a two-dimensional polymeric cluster with the cage structure that could be a promising candidate for an optical limiting material.

Spectroscopic Properties. Infrared and electronic spectra for **1**−**6** are normal compared with those for related compounds containing the $[WSe_4]^{2-}$ anion.[12,14−18] The W-Se stretching modes of these clusters can be identified easily because they appear as sharp peaks in the low−wavenumber region below 400 cm^{-1} in the IR spectrum. The terminal $W-Se_t$ absorption for **4** was found at 318 cm^{-1}, which is higher than that for the $[WSe_4]^{2-}$ anion (305 cm^{-1}).[1g] The bridging W−Se vibrations are observed in the range of 290−300 cm^{-1}, which is lower than that for $[WSe_4]^{2-}$.[18] The strong absorption at 913 cm^{-1} for **3** may be attributed to the terminal $W-O_t$ stretching vibration. The IR spectra of **2**, **3**, and **6** show bands in the range of 1557−1570 cm^{-1}, which can be obviously assigned to the ν(C−N) of the pyridine ligands.

The electronic absorption spectrum of each of these clusters shows several intense bands in the UV region with weaker bands in the visible region.These bands are not of the d−d type but probably result from ligand−metal charge transfer. Assignments of absorption bands for heteroselenometallic complexes with the $[WSe_4]^{2-}$ anion have been reported in the literature.[14−18, 29] On the basis of these assignments, the intense and weaker bands at 300−380 nm for clusters **1**−**6** may be attributed to the internal Se to W charge-transfer transition of the $[WSe_4]^{2-}$ moiety and the relatively weak ligand $[WSe_4]^{2-}$ to copper interaction, respectively.

The ^{1}H NMR spectra of clusters **2**, **3**, and **6** show one doublet and two triplet peaks from the protons of pyridine ligands. The ^{31}P NMR spectrum of cluster **4** shows a singlet at 26.4 ppm, which is comparable to those of related cubanelike clusters with PPh_3 ligands.[14] The FAB^+ mass spectra of clusters **2**−**4** and **6** exhibit molecular ions corresponding to $M^+ + 1$ and $M^+ -$ ligands with the characteristic isotopic distribution patterns. Although the parent molecular ions of clusters **1** and **5** are detected at very low intensity, a series of intense peaks assigned to ions which are formed by the subsequent loss of the iodide ligands were observed.

(24) (a) Cao, R.; Zhang, Q. F.; Su, W. P.; Bao, M. T.; Zheng, Y.; Hong, M. C. *Polyhedron* **1999**, *18*, 333. (b) Beheshti, A.; Brooks, N. R.; Clegg, W.; Sichani, S. E. *Polyhedron* **2004**, *23*, 3143.
(25) (a) Halbert, T. R.; Pan, W.-H.; Stiefel, E. I. *J. Am. Chem. Soc*. **1983**, *105*, 5476. (b) Pan, W.-H.; Chanlder, T.; Enemark, J. H.; Stiefel, E. I. *Inorg. Chem*. **1984**, *23*, 4265.
(26) Zhang, Q. F.; Zhang, C.; Song, Y. L.; Xin, X. Q. *J. Mol. Struct*. **2000**, *525*, 79.
(27) Sécheresse, F.; Bernes, S.; Robert, F.; Jeannin, Y. *Bull. Soc. Chim. Fr*. **1995**, *132*, 1029.
(28) (a) Hou, H. W.; Fan, Y. T.; Du. C. X.; Zhu, Y.; Wang, W. L.; Xin, X. Q.; Low, M. K. M.; Ji, W.; Ang, H. G. *Chem. Commun*. **1999**, 647. (b) Lang, J. P.; Xin, X. Q.; Yu, K. B. *J. Coord. Chem*. **1994**, *33*, 99.

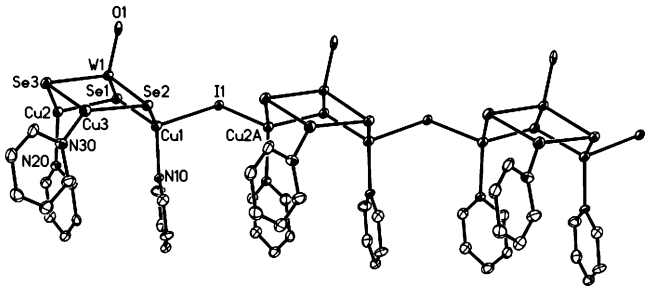

Figure 1. View of a $[(\mu_3\text{-}WOSe_3)Cu_3(py)_3(\mu\text{-}I)]_n$ (**3**) chain, three unit cells long drawn as an ORTEP diagram with 50% displacement ellipsoids. Only inequivalent atoms are labeled.

Table 2. Selected Bond Distances (Å) and Angles (deg) for $[(\mu_3\text{-}WOSe_3)Cu_3(py)_3(\mu\text{-}I)]_n$ (**3**)[a]

W(1)−O(1)	1.826(9)	W(1)−Se(1)	2.3865(13)
W(1)−Se(2)	2.4243(13)	W(1)−Se(3)	2.3993(16)
Cu(1)−Se(1)	2.4030(17)	Cu(1)−Se(2)	2.4091(18)
Cu(2)−Se(1)	2.430(2)	Cu(2)−Se(3)	2.4081(19)
Cu(3)−Se(2)	2.358(2)	Cu(3)−Se(3)	2.3655(18)
Cu(1)−N(10)	2.026(9)	Cu(1)−I(1)	2.702(2)
Cu(2)−N(20)	2.084(9)	Cu(2)−I(1)#1	2.6112(16)
Cu(3)−N(30)	1.945(10)	W(1)−Cu(1)	2.7421(17)
W(1)−Cu(2)	2.7953(16)	W(1)−Cu(3)	2.7091(19)
O(1)−W(1)−Se(1)	108.0(2)	O(1)−W(1)−Se(3)	109.5(2)
O(1)−W(1)−Se(2)	110.2(2)	Se(1)−W(1)−Se(3)	109.58(5)
Se(1)−W(1)−Se(2)	110.47(5)	Se(2)−W(1)−Se(3)	109.08(5)
W(1)−Se(1)−Cu(1)	69.85(5)	W(1)−Se(1)−Cu(2)	70.95(6)
W(1)−Se(2)−Cu(1)	69.13(5)	W(1)−Se(2)−Cu(3)	68.99(5)
W(1)−Se(3)−Cu(2)	71.11(6)	W(1)−Se(3)−Cu(3)	69.30(6)
Cu(1)−Se(1)−Cu(2)	107.16(7)	Cu(1)−Se(2)−Cu(3)	112.08(7)
Cu(2)−Se(3)−Cu(3)	107.01(7)	Se(1)−Cu(1)−Se(2)	110.43(7)
Se(1)−Cu(2)−Se(3)	107.85(7)	Se(2)−Cu(3)−Se(3)	112.56(7)
Se(1)−Cu(1)−I(1)	105.19(6)	Se(1)−Cu(2)−I(1)#1	111.11(6)
Se(2)−Cu(1)−I(1)	108.09(7)	Se(3)−Cu(2)−I(1)#1	109.98(6)
N(10)−Cu(1)−Se(1)	113.7(3)	N(10)−Cu(1)−Se(2)	115.5(3)
N(10)−Cu(1)−I(1)	103.1(3)	N(20)−Cu(2)−Se(3)	115.6(3)
N(20)−Cu(2)−Se(1)	105.0(3)	N(20)−Cu(2)−I(1)#1	107.3(3)
N(30)−Cu(3)−Se(2)	129.3(3)	N(30)−Cu(3)−Se(3)	116.6(3)
Cu(1)−I(1)−Cu(2)#2	109.71(6)		

[a] Symmetry code: #1 $x + 1, y, z$; #2 $x - 1, y, z$.

Crystal Structures. The structure of **3** has been established by an X-ray diffraction study. The molecular structure of **3** is shown in Figure 1, and selected bond lengths and angles are given in Table 2. The structure of **3** consists of an open nest-shaped WSe_3Cu_3 core linked by iodides to form a one-dimensional polymer. A similar $MoSe_3Cu_3$ core has been found for a related heteroselenometallic cluster, $[Ph_4P]_2[(\mu_3\text{-}MoOSe_3)Cu_3Cl_3(py)]$.[15] The center W atom has a nearly tetrahedral geometry with the angles around W atom ranging from 108.0(2) to 110.47(5)°. The W−O bond length of 1.826(9) Å is typical for a W═O double bond. The average W−μ_3-Se bond length in **3** is 2.4034(14) Å. There are two kinds of Cu atoms: (a) the tetrahedral Cu atoms coordinated to two Se, one I, and one N of py and (b) the trigonal Cu atom coordinated to two Se and one N of py. The W−Cu separations involving tetrahedral Cu (2.7953(16) and 2.7421(17) Å) are longer than that involving trigonal Cu (2.7091(19) Å). The bond lengths between the bridging I atom and two Cu atoms are 2.702(2) and 2.6112(16) Å. The Cu−I−Cu linkage in the polymer is bent with an angle of 109.71(6)°.

The structure of **5** consists of well-separated cations and anions. The structure of the $[(\mu_5\text{-}WSe_4)(CuI)_5(\mu\text{-}I)_2]^{4-}$ anion

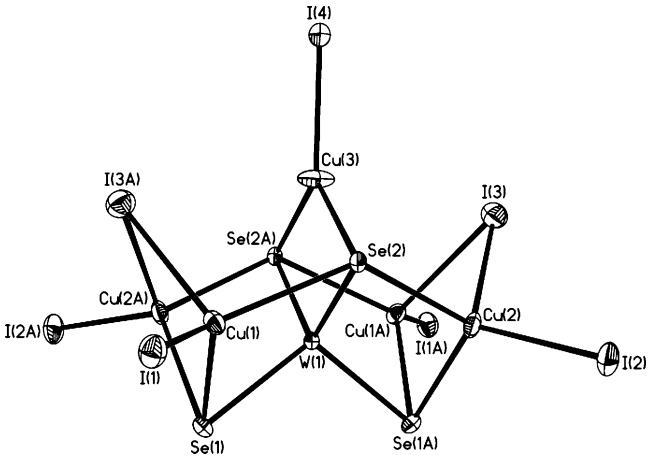

Figure 2. Molecular structure of the cluster anion of **5**, showing 50% thermal ellipsoids.

Table 3. Selected Bond Distances (Å) and Angles (deg) for $[Et_4N]_4[(\mu_5\text{-}WSe_4)(CuI)_5(\mu\text{-}I)_2]$ (**5**)[a]

W(1)−Se(1)	2.3513(11)	W(1)−Se(2)	2.3950(12)
Cu(1)−Se(1)	2.4228(18)	Cu(1)−Se(2)	2.4643(18)
Cu(2)#1−Se(1)	2.4182(19)	Cu(2)−Se(2)	2.4542(18)
Cu(3)−Se(2)	2.3748(16)	Cu(1)−I(1)	2.4350(18)
Cu(1)−I(3)#1	2.6641(19)	Cu(2)−I(2)	2.441(2)
Cu(2)−I(3)	2.672(2)	Cu(3)−I(4)	2.425(3)
W(1)−Cu(1)	2.7516(16)	W(1)−Cu(2)	2.7420(17)
W(1)−Cu(3)	2.725(2)		
Se(1)#1−W(1)−Se(1)	105.66(6)	Se(1)−W(1)−Se(2)#1	110.40(4)
Se(1)−W(1)−Se(2)	110.36(4)	Se(2)#1−W(1)−Se(2)	109.61(6)
W(1)−Se(1)−Cu(2)#1	70.17(5)	W(1)−Se(1)−Cu(1)	70.37(5)
W(1)−Se(2)−Cu(1)	68.96(5)	W(1)−Se(2)−Cu(2)	68.85(5)
Cu(2)#1−Se(1)−Cu(1)	81.38(7)	Cu(3)−Se(2)−W(1)	69.69(6)
Cu(3)−Se(2)−Cu(2)	96.05(6)	Cu(3)−Se(2)−Cu(1)	95.74(6)
Cu(2)−Se(2)−Cu(1)	128.55(7)	Se(1)−Cu(1)−Se(2)	105.74(7)
Se(1)#1−Cu(2)−Se(2)	106.24(7)	Se(1)−Cu(1)−I(3)#1	100.66(7)
Se(2)#1−Cu(3)−Se(2)	111.01(10)	Se(1)−Cu(1)−I(1)	119.96(7)
I(1)−Cu(1)−Se(2)	119.19(8)	I(1)−Cu(1)−I(3)#1	106.50(7)
Se(2)−Cu(1)−I(3)#1	101.59(6)	Se(1)#1−Cu(2)−I(2)	118.45(7)
I(2)−Cu(2)−Se(2)	117.98(8)	Se(1)#1−Cu(2)−I(3)	100.57(7)
I(2)−Cu(2)−I(3)	109.58(7)	Se(2)−Cu(2)−I(3)	101.32(6)
Se(2)−Cu(3)−I(4)	124.50(5)	Cu(1)#1−I(3)−Cu(2)	72.52(6)

[a] Symmetry code: #1 $-x + 1, y, -z + 1/2$.

in **5** is illustrated in Figure 2, and selected bond lengths and angles are given in Table 3. The $[(\mu_5\text{-}WSe_4)(CuI)_5(\mu\text{-}I)_2]^{4-}$ anion comprises two $[(CuI)_2(\mu\text{-}I)]$ fragments symmetrically ligated to the tetrahedral $[WSe_4]^{2-}$ moiety and one CuI species occupying one face of the WSe_4Cu_4 core, forming a crownlike overall structure. The W(1), Cu(3), and I(4) atoms lie on a crystallographic 2-fold axis. The central W atom has a slightly distorted tetrahedral coordination geometry with the Se−W−Se angles ranging from 105.66(6) to 110.40(4)°. The W−Se bond length involving μ_4-Se (2.3950(12) Å) is slightly longer than that involving μ_3-Se (2.3513(11) Å). The four Cu atoms, Cu(1), Cu(2), Cu(1A), and Cu(2A), are nearly coplanar with a deviation of 0.0057 Å from the least-squares plane. Compared with the coplanar WCu_4 cores in the open-squared clusters $[(\mu_4\text{-}WSe_4)Cu_4(py)_6Cl_2]$,[12b] $[Et_4N]_2[(\mu_4\text{-}WSe_4)Cu_4(S_2CNMe_2)_4]$,[16b] and $\{[Et_4N]_2[(\mu_4\text{-}WSe_4)Cu_4(CN)_4]\}_n$,[18a] the W atom in **5** is deviated from the Cu_4 plane with a distance of ca. 0.38 Å because of an extra CuI species binding to one of WSe_2 faces. Similar to **3**, the W−Cu(tetrahedral) separations of 2.7516(16) and 2.7420-

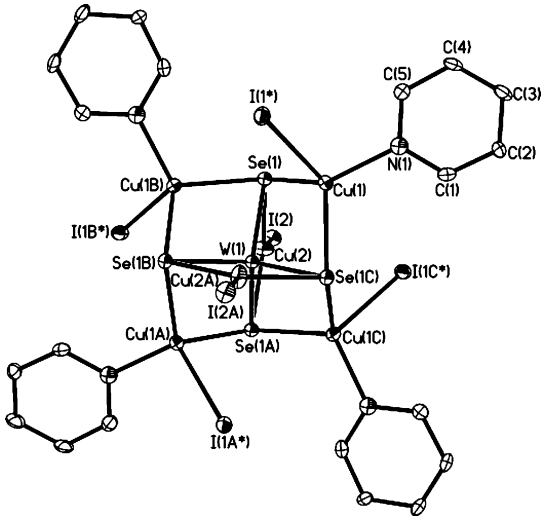

Figure 3. View of the molecular structure of $[(\mu_6\text{-}WSe_4)Cu_6I_4(py)_4]$ as a repeating unit in **6**. Displacement ellipsoids are plotted at the 50% probability level.

(17) Å are significantly longer than that (2.725(2) Å) involving the trigonal Cu in **5**, suggesting that the interactions between the W and Cu are greatly influenced by the coordination geometry of Cu. There are two types of geometry about the Cu atoms: (i) distorted tetrahedral with angles varying from 101.32(6) to 119.96(7)° and (ii) distorted trigonal with angles ranging from 111.01(10) to 124.50(5)°. The average $Cu-I_t$ and $Cu-I_b$ bond lengths in **5** are 2.434(2) and 2.668(2) Å, respectively, and are similar to those of related compounds.[23,28a,30]

The solid-state structure of **6** has been established by X-ray crystallography. Although a similar structure has been found for the heterothiometallic clusters $[(\mu_6\text{-}MoS_4)Cu_6X_4(py)_4]_n$ (X = Br, I),[28] the current arrangement appears to the first example of an octahedral polymeric cluster containing a tetraselenometalate moiety. The basic octahedral unit $[(\mu_6\text{-}WSe_4)Cu_6I_4(py)_4]$ is illustrated in Figure 3, and selected bond lengths and angles are given in Table 4. The structure possesses a crystallographic D_{2d} symmetry. The basic core WSe_4Cu_6 is formed of a central WSe_4 tetrahedron encapsulated by six Cu atoms across six faces of the WSe_2 type. The central WSe_4 retains an idealized tetrahedral geometry with the average Se−W−Se bond angle of 109.26(2)° and a W−μ_4-Se bond length of 2.3986(6) Å. The six Cu atoms form a regular octahedral array. The Cu−Se bond lengths are obviously inequivalent: the Cu−Se bond distances for tetrahedral Cu atoms are 2.4342(11) and 2.4005(12) Å, whereas that for the trigonal Cu atom is 2.3578(10) Å. The W−Cu(tetrahedral) separation of 2.7396(9) Å is slightly longer than that involving the trigonal Cu atoms (2.7276(15) Å). The average W−Cu separation in **6** (2.7336(12) Å) is comparable to those in **3** (2.7488(17) Å), **5** (2.7395(18) Å), and other related clusters.[12,17,18] The average $Cu-I_t$ and $Cu-I_b$ bond lengths in **6** are 2.4613(16) and 2.6838(11) Å, respectively, which are comparable to those in **5**. The angles around the tetrahedral Cu atoms range from 95.16(4) to 114.2(2)°, suggesting that the coordination geometry of the Cu atoms is highly distorted tetrahedral. It is significant to note that the Cu−I−Cu angle of 108.60(5)° in **6** is similar to that in **3** (109.71(6)°). This, together with the observation of the smallest $Se-Cu-I_b$ angle of 95.16(4)° in the tetrahedral Cu coordination environment, makes the four bridging I atoms connect to four tetrahedral Cu atoms of each octahedral $[(\mu_6\text{-}WSe_4)Cu_6I_4(py)_4]$ unit, leading to the construction of a two-dimensional network polymeric cluster, as shown in Figure 4.

Table 4. Selected Bond Distances (Å) and Angles (deg) for $[(\mu_6\text{-}WSe_4)Cu_6I_4(py)_4]_n$ (**6**)[a]

W(1)−Se(1)	2.3986(6)	Cu(1)−Se(1)	2.4342(11)
Cu(1)−Se(1)#2	2.4005(12)	Cu(2)−Se(1)	2.3578(10)
Cu(1)−I(1)	2.6838(11)	Cu(2)−I(2)	2.4613(16)
Cu(1)−N(1)	1.984(7)	W(1)−Cu(1)	2.7396(9)
W(1)−Cu(2)	2.7276(15)		
Se(1)−W(1)−Se(1)#1	109.898(16)	Se(1)−W(1)−Se(1)#3	108.62(3)
W(1)−Se(1)−Cu(1)#1	69.62(3)	W(1)−Se(1)−Cu(1)	69.06(3)
W(1)−Se(1)−Cu(2)	69.98(3)	Cu(1)−Se(1)−Cu(1)#1	107.95(3)
Cu(1)−Se(1)−Cu(2)	118.62(4)	Cu(2)−Se(1)−Cu(1)#1	98.05(4)
Se(1)−Cu(1)−Se(1)#2	108.64(4)	Se(1)−Cu(2)−Se(1)#3	111.43(6)
Se(1)−Cu(1)−I(1)	95.16(4)	Se(1)#2−Cu(1)−I(1)	109.61(4)
Se(1)−Cu(2)−I(2)	124.29(3)	N(1)−Cu(1)−Se(1)#2	114.2(2)
N(1)−Cu(1)−Se(1)	122.8(2)	N(1)−Cu(1)−I(1)	103.9(2)
Cu(1)−I(1)−Cu(1)#4	108.60(5)		

[a] Symmetry code: #1 $y, -x, -z$; #2 $-y, x, -z$; #3 $-x, -y,$ z; #4 $-x + 1/2, y, -z - 1/4$.

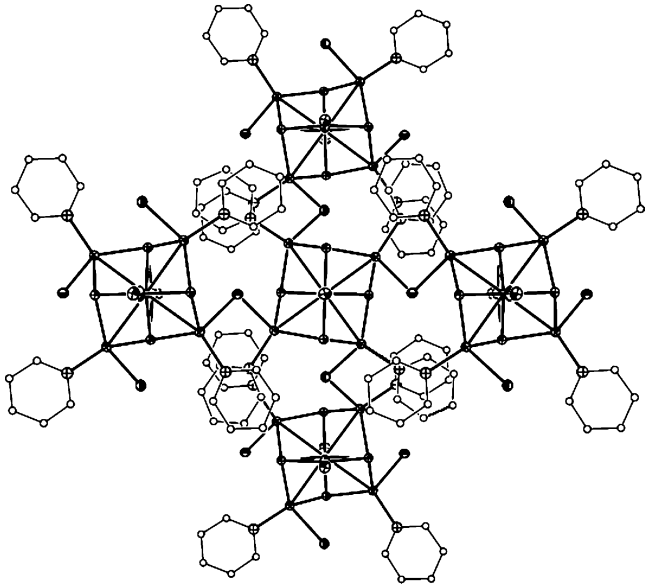

Figure 4. Perspective view of the two-dimensional structure of $[(\mu_6\text{-}WSe_4)Cu_6I_4(py)_4]_n$ along the *c* axis.

Optical Limiting Effect. According to the previous studies, structure alternation and the skeleton atom substitution can induce larger variations in the NLO properties of heterobimetallic sulfido and selenido clusters.[6,7,18,31] Of interest are polynuclear cage-shaped and polymeric clusters that exhibit strong nonlinear optical absorption and refraction,

(29) Ansari, M. A.; Chau, C.-N.; Mahler, C. H.; Ibers, J. A. *Inorg. Chem.* **1989**, *28*, 650.

(30) (a) Hou, H. W.; Long, D. L.; Xin, X. Q.; Huang, X. Y.; Kang, B. S.; Ge, P.; Ji, W.; Shi, S. *Inorg. Chem.* **1996**, *35*, 5363. (b) Li, J. G.; Gao, F. J.; Lang, J. P.; Xin, X. Q.; Chen, M. Q. *Chin. J. Struct. Chem.* (*Jiegou Huaxue*) **1992**, *11*, 351.

(31) Zhang, Q. F.; Song, Y.; Wong, W. Y.; Leung, W. H.; Xin, X. *J. Chem. Soc., Dalton Trans.* **2002**, 1963.

along with especially strong optical limiting effects. For examples, cubanelike clusters $[(\mu_3\text{-}MSe_4)M'_3(PPh_3)_3(\mu_3\text{-}Cl)]$ (M = Mo, W; M′ = Cu, Ag),[7b,14e] hexagonal prism-shaped cluster $[Mo_2Ag_4S_8(AsPh_3)_4]$,[32] two-dimensional octahedral cluster polymer $[MoS_4Cu_6I_4(py)_4]_n$,[28a] three-dimensional open-cross cluster polymer $\{[Et_4N]_2[(\mu_4\text{-}WSe_4)Cu_4(CN)_4]\}_n$,[18a] and two-dimensional polymeric cluster $\{[Et_4N][Mo_2O_2S_6Cu_6I_3(4,4'\text{-bipy})_5]\cdot MeOH\cdot H_2O\}_n$[5g] show large optical limiting effects with relatively lower optical limiting thresholds. On the basis of these results, we sought to synthesize the tailored cluster $[(\mu_6\text{-}WSe_4)Cu_6I_4(py)_4]_n$ with an octahedral cage core structure for the further investigation of its NLO properties with the expectation that polynuclear polymeric clusters would possess a large optical limiting effect.

Cluster **6** was dissolved in DMSO with a nonsaturation concentration of 2.25×10^{-5} mol dm^{-3} and put in a 1 mm thick glass cell for optical limiting measurements. The linear transmissivity of the sample is 78% at 532 nm, corresponding to a ground-state absorption cross section of 1.8×10^{-18} cm^2. For comparison, a solution of C_{60} in toluene with the same linear transmissivity was measured under the same experimental conditions.[33] To obtain the NLO parameters, we employed a *z* scan theory[21] that considers effective nonlinearity of third-order nature only: $\alpha = \alpha_0 + \alpha_2 I$ and $n = n_0 + n_2 I$, where α_0 and α_2 are the linear and nonlinear absorption coefficient, respectively; n_0 and n_2 are the linear and nonlinear refractive index, respectively; and I is the irradiance of the laser beam within the sample. The peak fluence for the *z* scan is about 1 J dm^{-2} both in nanosecond *z* scans. The α_2 and n_2 values extracted from 7 ns experimental data are 2.9×10^{-5} m W^{-1} M^{-1} and -3.6×10^{-12} m^2 W^{-1} M^{-1}, respectively. The strong nonlinear absorptivity and the nonlinear refractive self-defocusing behavior of **6** are comparable to those of $[Mo_2Ag_4S_8(AsPh_3)_4]$,[32] $\{[Et_4N]_2[(\mu_4\text{-}WSe_4)Cu_4(CN)_4]\}_n$,[18a] and $\{[Et_4N][Mo_2O_2S_6Cu_6I_3(4,4'\text{-bipy})_5]\cdot MeOH\cdot H_2O\}_n$[5g] but are superior to those of the analogous sulfur cluster $[MoS_4Cu_6I_4(py)_4]_n$,[28a] possibly because of the heavy atom effect.

The optical limiting phenomenon was also observed by measuring the nonlinear (energy-dependent) transmission. An aperture was placed in front of the transmission detector when the measurement was performed. Figure 5 represents the observed variation of output fluence with input fluence for cluster **6** in DMSO and C_{60} in toluene. It is clear that the optical limiting capability of the cluster is better than that of C_{60} with the same linear transmissivity.[34] The optical limiting threshold, defined as the input fluence at which the transmissivity is 78% of the linear transmissivity is about 0.30 J cm^{-2} for the cluster compound and about 0.60 J cm^{-2} for C_{60}. When the incident fluence exceeds 0.1 J cm^{-2}, the solution transmittance decreases as the incident fluence is increased, thus exhibiting a typical optical limiting effect.

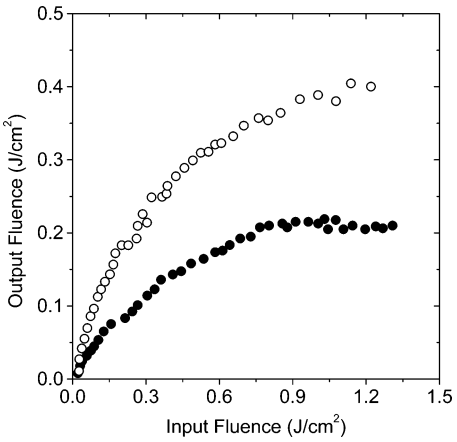

Figure 5. Optical limiting effect of **6** (2.25×10^{-5} mol dm^{-3} in DMSO, ●) and C_{60} (6.25×10^{-4} mol dm^{-3} in toluene, ○).

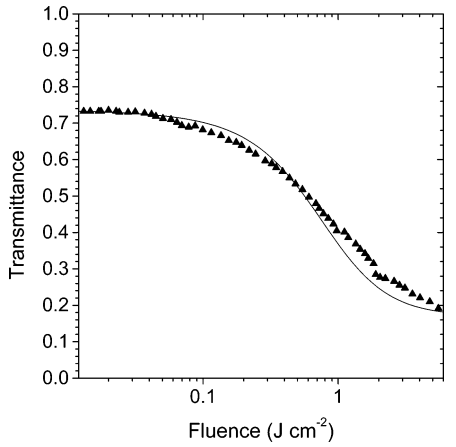

Figure 6. Energy-dependent transmittance of a $[(\mu_6\text{-}WSe_4)Cu_6I_4(py)_4]_n$ DMSO solution (2.25×10^{-5} mol dm^{-3}) on the incident light fluence. Optical path: 1 mm. Laser wavelength: 532 nm. Pulse duration: 7 ns. Repetition rate: single shot (10 s interval).

The optical limiting performance with repetition rate at single shots (10 s interval) is also displayed in Figure 6, from which we determined the limiting threshord in a DMSO solution to be ca. 0.28 J cm^{-2}. Within the experimental error, no significant difference was found among measurements, thereby indicative of cluster **6** having good photostability.[35] Further support for the stability of **6** is the fact that the sample remained effective and its electronic spectrum remained unchanged even if the sample was prepared several weeks ago. Obviously, the optical limiting capability of the octahedral polymeric cluster **6** is comparable to that of cross-framework polymeric clusters $\{[Et_4N]_2[(\mu_4\text{-}MQ_4)Cu_4(CN)_4]\}_n$ (M = Mo, W; Q = S, Se),[18] nest-shaped 2D polymeric cluster $\{[Et_4N][Mo_2O_2S_6Cu_6I_3(4,4'\text{-bipy})_5]\cdot MeOH\cdot H_2O\}_n$,[5g] and open-cross 3D polymeric cluster $\{[(WS_4)(Cu4,4'\text{-bipy})_4][(WS_4)(CuI4,4'\text{-bipy})_4]\}_n$;[5b] it may therefore provide a proof that polymeric aggregation of heterobimetallic sulfur and selenide clusters may result in enhancement of the optical limiting effect.

In summary, we have investigated the cluster skeleton's transformation of the coplanar cluster $[Et_4N]_4[(\mu_4\text{-}WSe_4)$-

(32) Sakane, G.; Shibahara, T.; Hou, H. W.; Xin, X. Q.; Shi, S. *Inorg. Chem.* **1995**, *34*, 4785.
(33) Mclean, D. G.; Sutherland, R. L.; Brant, M. C.; Brandelik, D. M.; Fleitz, P. A.; Pottenger, T. *Opt. Lett.* **1993**, *18*, 858.
(34) (a) Tutt, L. W.; Kost, A. *Nature* **1992**, *356*, 225. (b) Henari, F.; Callaghan, J.; Stiel, H.; Blau, W.; Cardin, D. J. *Chem. Phys. Lett.* **1992**, *199*, 144.
(35) (a) Ji, W.; Xie, W.; Tang, S. H.; Shi, S. *Mater. Chem. Phys.* **1996**, *43*, 45. (b) Ji, W.; Du, H. J.; Tang, S. H.; Shi, S. *J. Opt. Soc. Am. B* **1995**, *12*, 876.

Cu_4I_6] under different reaction conditions. Binding of Cu(I) ions to the two uncoordinated MSe_2 edges of the coplanar MSe_4Cu_4 core in **1** led to the formation of two new cluster compounds, namely, $[Et_4N]_4[(\mu_5\text{-}WSe_4)(CuI)_5(\mu\text{-}I)_2]$ with a crown-like structure and polymeric $[(\mu_6\text{-}WSe_4)Cu_6I_4(py)_4]_n$ with an octahedral WSe_4Cu_6 repeating unit. It is believed that the cage core structure of octahedral polymeric $[(\mu_6\text{-}WSe_4)Cu_6I_4(py)_4]_n$ contributes to its good photostability, along with the large optical limiting effect. The design and syntheses of new heteroselenometallic clusters based on this synthetic method is in active progress in this laboratory.

Acknowledgment. This project was supported by the Natural Science Foundation of China (90301005) and the Hong Kong Research Grants Council. Q.-F.Z. thanks the Science and Technological Fund of Anhui Province for Outstanding Youth (06046100) and the Alexander von Humboldt Foundation for assistance.

Supporting Information Available: Crystallographic data for compounds **3**, **5**, and **6** in CIF format. This material is available free of charge via the Internet at http://pubs.acs.org.

IC060161P